POLISH MARITIME RESEARCH 2 (118) 2023 Vol. 30; pp. 105-113
10.2478/pomr-2023-0026

BEHAVIOUR OF A TORSIONAL VIBRATION VISCOUS DAMPER IN THE EVENT OF A DAMPER FLUID SHORTAGE

Andrzej Chmielowiec*
Rzeszow University of Technology, Poland
Adam Michajłyszyn
Rzeszow University of Technology, Poland
Wojciech Homik
Rzeszow University of Technology, Rzeszow, Poland

* Corresponding author: *achmie@prz.edu.pl (Andrzej Chmielowiec)*

ABSTRACT

Abstract: This article presents the analysis of a damping fluid deficiency in a torsional vibration viscous damper. The problem is analysed both qualitatively and quantitatively. Experimental results are presented, showing what happens to the damper in a situation where the design of the housing is inadequate and the inertia forces prevent the formation of an oil film. In addition, the article deals with the problem of the proper design of the oil channel and the dimensions required to enable the damper to operate reliably. The results of the article may be useful to the constructors of torsional vibration viscous dampers for marine engines.

Keywords: ngine vibrations; Torsional vibration; Viscous damper; Oil channel; Damper design

INTRODUCTION

The problem of vibrations and their damping occurs in all types of internal combustion engine. In these engines, the reciprocating motion is converted into rotational motion by means of a piston-crank system. During this process, the engine's crankshaft is affected by gas forces arising in the combustion process of the fuel-air mixture and inertia forces originating from the masses in motion. Periodic changes in force generates vibrations in the entire system, the most dangerous of which are torsional vibrations [2, 8, 18]. This problem particularly concerns large engines, especially ships' engines, for which the above-mentioned loads may even lead to engine destruction in extreme conditions. This is evidenced by numerous publications reporting damage to crankshafts in marine engines. In recent years, such events have been described, among others, by Fonte et al. [5, 6], Gomes et al. [7] and Kutay and Kamal [16]. Contemporary failures motivated scientists to develop risk assessments related to torsional vibrations of ship propulsion systems. Liberacki [17] defined the risk associated with crankshaft failure and Senjanović et al. [22] and Murawski and Dereszewski [19] presented methods for assessing and monitoring torsional vibrations in a ship's power plant. To address issues associated with the generation of torsional vibrations, a properly selected damper should be installed as a solution. In the case of marine engines, the dominant device is a viscous torsional vibration damper [10]. The authors Komada and Honda [14, 15], Dziurdź and Pakowski [4], Pasricha [20] and Homik [11] all described the characteristics of the damper operation and its impact on the amplitude of torsional vibrations in the propulsion system of a ship. The conditions for the reliable operation of a torsional vibration viscous damper is the formation of

an oil film between the housing and the inertial ring. Such an oil film makes it possible to dissipate energy through internal friction in fluid particles, with no wearing of the damper parts. Considering the above, it should be stated that one important issue is the level to which the damper is filled with fluid of an appropriate viscosity. The right level of filling ensures effective and reliable operation. Improper, or too little, filling of the damper causes accelerated wear on the active surfaces, which reduces its effectiveness. In connection with the above, constructors use various types of procedures that allow this problem to be solved. One solution is to reduce wear by using appropriate materials [1, 9]. The second solution is to ensure fluid friction through the correct design of the oil channel.

This article presents the behaviour of silicone oil during the start-up of a torsional vibration viscous damper. Formulas for the volume of the oil channel have also been determined, the proper execution of which guarantees the formation of the oil film carrier layers. The information contained herein may be useful for the constructors of torsional vibration viscous dampers for marine engines.

DESIGN AND PRINCIPLE OF TORSIONAL VIBRATION VISCOUS DAMPER OPERATION

The torsional vibration viscous damper is a relatively simple device in its design and its individual parts are shown in Fig. 1. The basic elements responsible for its proper functioning are: housing connected to the cover, an inertia ring and silicone oil. The interaction of these three parts makes it possible to dissipate the energy of torsional vibrations in the form of heat. In Fig. 1, the oil channel (item 8) is highlighted. This element is often overlooked in various types of torsional vibration viscous damper analysis. This article shows that the oil channel is a key element, from the point of view of proper functioning of the device.

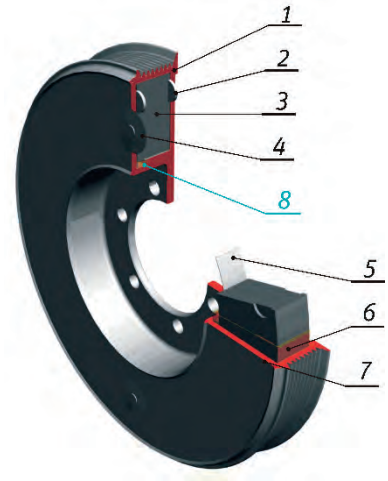

Fig. 1. Torsional vibration viscous damper: 1 - damper housing, 2 - thrust bearing, 3 - inertia ring, 4 - plug, 5 - radial bearing, 6 - silicone oil, 7 - cover, 8 - oil channel.

The essence of the effective operation of a torsional vibration viscous damper is the relative movement of the inertia ring and the housing. This movement is shown in Fig. 2, by the angular velocity of the housing ω_H and the angular velocity of the inertia ring ω_I. If only $\omega_H \neq \omega_H$, then the viscosity of the fluid between the ring and the housing creates a frictional force. This force is proportional to the speed difference between the housing and the inertia ring at a given point, and inversely proportional to the distance between them. This mechanism creates a braking force that counteracts sudden changes in the angular velocity of the housing. This makes it possible to suppress torsional vibrations. Fig. 2 shows a diagram of a working torsional vibration viscous damper. All of the necessary geometric properties are marked on it, which allow description of the movement of the ring, assuming that the empty spaces are completely filled with silicone oil.

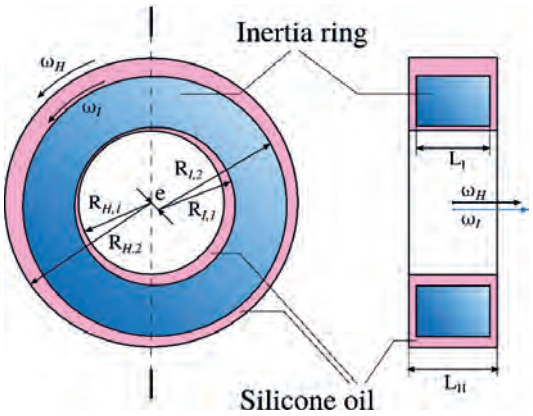

Fig. 2. Overview of a torsional vibration viscous damper, in which the inertial ring rotates with an angular velocity ω_I, the housing rotates with an angular velocity ω_H, and the eccentricity of the housing and the inertia ring has the value e.

It is worth noting that the radial internal clearance $c_1 = R_{l,1} - R_{H,1}$ is smaller than the external radial clearance $c_2 = R_{H,2} - R_{I,2}$. The c_2/c_1 ratio is generally so large that the weight of the ring is mainly supported by the hydrodynamic force generated in the inner oil layer. To generate this hydrodynamic lift, (poly)dimethylsiloxane is used, which is characterised by high viscosity. Depending on the application, its kinetic viscosity generally varies from 10,000 cSt (0.01 m^2s^{-1}) to 1,000,000 cSt (1 m^2s^{-1}). Such large values are obtained by creating very long polymer chains, the structure of which is shown in Fig. 3.

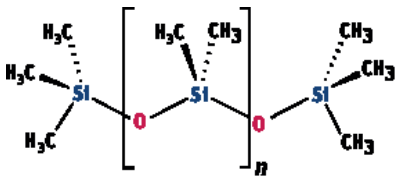

Fig. 3. Structural formula of a silicone oil molecule - (poly)dimethylsiloxane, whose viscosity is closely related to the length of the chain of repeating dimethyl groups [3].

The aforementioned viscosities require the synthesis of chains consisting of 500 to 2,000 dimethyl groups. In addition, this type of fluid is characterised by highly variable viscosity, as afunction of temperature. As shown in [3], the (poly) dimethylsiloxanes used in damping devices differ in their characteristics from the commonly used models of viscosity as a function of temperature. Another very important feature of silicone oil is its relative volumetric expansion ($930 \cdot 10^{-6}$ per °C), i.e. about 4.5 times the volumetric expansion of water. This means that, in the operating temperature range from –30 °C to about 70 °C, its volume changes by about 10%. Thus, there is never a situation in which the damper is completely filled with viscous fluid. This is the main reason for using an oil channel in the design of the damper. It is intended as a kind of buffer into which excess oil is drained during operations at high temperatures and from which it is drawn during operations at low temperatures. The main task of the channel is to provide oil in the layer between the radii $R_{H,1}$ and $R_{I,1}$, which is the main carrying layer for the inertia ring. A lack of oil in this layer causes dry friction and mixed friction (dry and wet) between the housing and the inertia ring. This leads to the wear of inner damper surfaces and contamination of the oil. In addition, such a damper loses its damping properties and, in extreme cases, may even act as a vibration exciter.

HYDRODYNAMIC FORCES IN THE DAMPER

In order for the damper to fulfill its task, it is necessary to lift the ring by hydrodynamic forces. To model this phenomenon, a method based on the bearings theory is adopted [12]. The basis of this theory is the Reynolds equation [21] which, among other things, assumes laminar fluid flow. As evidenced by the experimental results discussed later in the article, the relative velocity between the inertia ring and the housing is small. Therefore, it was assumed that the movement of the fluid is laminar and the hydrodynamic pressure of the oil film is described by the formula

$$p(\varphi_i) = p_0 + 6\eta|\omega_H - \omega_I|\left(\frac{R_i}{c_i}\right)^2 \frac{\varepsilon_i(2+\varepsilon_i\cos\varphi_i)\sin\varphi_i}{(2+\varepsilon_i^2)(1+\varepsilon_i\cos\varphi_i)^2} \quad (1)$$

where φ_i is the angular coordinate shown in Fig. 5, p_0 is the pressure of the air enclosed in the housing, η is the dynamic viscosity of the silicone oil, R_i is, in accordance with the Reynolds condition, set to $\frac{1}{2}(R_{H,i} + R_{I,i})$, c_i is the radial clearance defined in the previous parts, and ε_i is the relative eccentricity, defined as the ratio e/c_i. It is worth noting here that adopting such a formula for R_i is purely arbitrary. The values of the radii $R_{H,i}$ and $R_{I,i}$ are so close that one may as well assume $R_i = R_{H,i}$ or $R_i = R_{I,i}$ as it will not have a significant impact on the obtained numerical results. By introducing the dimensionless function

$$\gamma(\varepsilon_i, \varphi_i) = \frac{\varepsilon_i(2+\varepsilon_i\cos\varphi_i)\sin\varphi_i}{(2+\varepsilon_i^2)(1+\varepsilon_i\cos\varphi_i)^2} \quad (2)$$

we get the following relation

$$p(\varphi_i) = p_0 + 6\eta|\omega_H - \omega_I|\left(\frac{R_i}{c_i}\right)^2 \gamma(\varepsilon_i, \varphi_i) \quad (3)$$

In accordance with the Gümbel condition, we now assume that the distribution of pressure in the inner ($i = 1$) and outer ($i = 2$) layers is given by the formula

$$p_i(\varphi_i) = \begin{cases} p(\varphi_i), & \varphi_i \in [0, \pi], \\ 0, & \varphi_i \in (\pi, 2\pi) \end{cases} \quad (4)$$

The behaviour of the hydrodynamic pressure function p_i is strictly dependent on the course of the dimensionless function $\gamma(\varepsilon_i,\varphi_i)$. This function, for several selected values of ε_i, is presented on the graph in Fig. 4. This graph presents a good picture of how the silicone oil pressure is distributed in the inner and outer layers. Note that the pressure function has exactly one maximum. By equating the derivative $\rho(\varphi_i)'$ to zero, it can be shown that this maximum is realised for a certain angle $\varphi_{i,m}$, satisfying the following relations

$$\sin(\varphi_{i,m}) = \frac{\left[(\varepsilon_i^2-1)(\varepsilon_i^2-2)\right]^{1/2}}{\varepsilon_i^2+2} \quad (5)$$

$$\cos(\varphi_{i,m}) = \frac{-3\varepsilon_i}{\varepsilon_i^2+2} \quad (6)$$

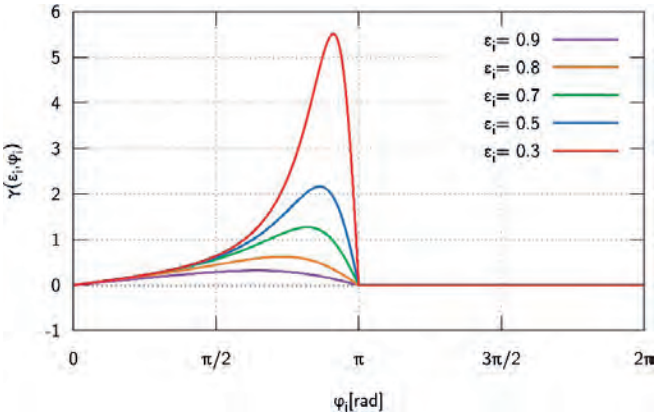

Fig. 4. Graph of the dimensionless function $\gamma(\varepsilon_i,\varphi_i)$ according to the Gümbel condition for example values of ε_i

By integrating the pressure of the inner layer p_1 and the pressure of the outer layer p_2 around the circumference of the inertia ring, we obtain the values of hydrodynamic forces acting on the inertia ring. During the operation of the damper, these forces are set at a level and in a position that balances the weight of the inertia ring. This situation is illustrated in Fig. 5, where the angle θ is the deviation angle of the axis $\varphi_i = 0$ from the vertical. Thus, in the equilibrium, the angle θ and the relative eccentricities ε_i must satisfy the relations

$$Q\cos\theta = -L_I R_1 \int_0^{2\pi} p_1 \cos\varphi_1 \, d\varphi_1 - L_I R_2 \int_0^{2\pi} p_2 \cos\varphi_2 \, d\varphi_2 \quad (7)$$

$$Q\sin\theta = L R_1 \int_0^{2\pi} p_1 \sin\varphi_1 \, d\varphi_1 + L R_2 \int_0^{2\pi} p_2 \sin\varphi_2 \, d\varphi_2 \quad (8)$$

By integrating by parts we get the following relations

$$Q\cos\theta = 12\eta|\omega_H - \omega_I|L_I \sum_{i=1}^{2} \frac{\varepsilon_i^2 R_i^3}{(2+\varepsilon_i^2)(1-\varepsilon_i^2)c_i^2} \quad (9)$$

$$Q\sin\theta = 6\pi\eta|\omega_H - \omega_I|L_I \sum_{i=1}^{2} \frac{\varepsilon_i R_i^3}{(2+\varepsilon_i^2)(1-\varepsilon_i^2)^{1/2} c_i^2} \quad (10)$$

It is true that three variables θ, ε_1 and ε_2 appear in the above equations, but the latter two are related by the equation $\varepsilon_1 = \varepsilon_2 \frac{c_2}{c_1}$. This means that Eqs. (9) and (10) give complete information about the equilibrium position of the inertia ring.

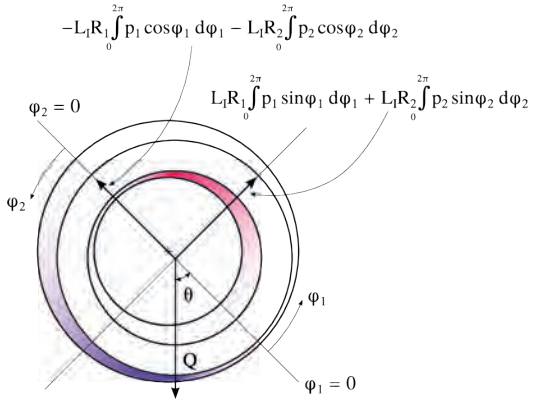

Fig. 5. Hydrodynamic forces balancing the weight of the inertia ring Q, given by the Gümbel condition for rotating elements (the intensity of the colour reflects the magnitude of the hydrodynamic pressure).

The adopted model does not take into account the movement of the fluid in the axial direction. Its great advantage, however, is the fact that it has analytical solutions and this makes it possible to quickly estimate the hydrodynamic pressure in both load-bearing layers. In future, the two-dimensional Reynolds equation may be used. Although it does not have analytical solutions, it will probably give a better picture of what is happening with the oil film inside the damper. Unfortunately, at the moment the authors do not have sufficient experimental data to determine reasonable boundary conditions for the numerical model.

DAMPER BEHAVIOUR IN THE CASE OF OIL SHORTAGE

Analysis of the torsional vibration viscous damper was performed on a specially prepared stand. This stand was first equipped with a damper designed with an error. This error consisted of the lack of an oil channel. In addition, the damper was deprived of bearings. This element was deliberately eliminated so that, during the experiments, it was possible to detect the difference in the operation of the damper without an oil channel and with an oil channel.

a) *b)*

Fig. 6. Position of silicone oil and air inside the damper: a) before starting work, b) after the oil is pushed out by the centrifugal force and the pressure of the inertia ring during operation.

Fig. 6a shows how the silicone oil fills the inside of the damper housing after 24 hours of rest in the vertical position. In contrast, Fig. 6b shows the position of the oil after only 3 minutes of damper operation. The photographs clearly show the displacement of the silicone oil in the circumferential direction due to the centrifugal force. Due to the lack of an oil channel, the inner support layer is stripped of oil and the inertia ring and housing are put into a dry and mixed friction state. After the tests, the damper housing was reworked and an oil channel was made in it. The modified damper was subjected to the same series of tests as the version without an oil channel. The cross-sections of the housing of both versions of the damper are shown in Fig. 7. The experiments clearly showed how important the oil channel is in the design. Its appropriate geometry guarantees the presence of silicone oil in both carrier layers, enabling the proper operation of the damper.

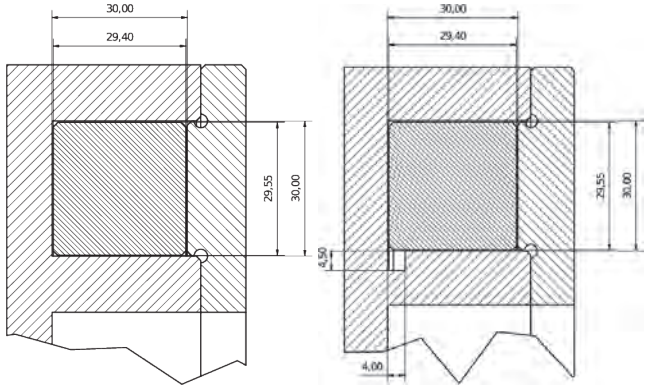

a) *b)*

Fig. 7. Damper model: a) without oil channel, b) with oil channel.

The results of the conducted experiments show which geometrical parameters of the damper are the most important, from the point of view of operational modelling, and they are shown in Fig. 8. The diagram includes two hydrodynamic pressures in both carrying layers and the pressure generated by the inertia force.

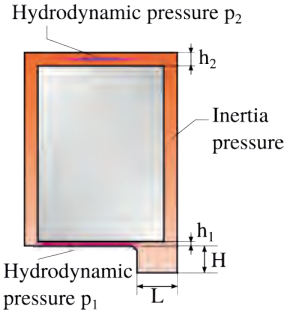

Fig. 8. Diagram of the oil channel's geometrical parameters in the torsional vibration viscous damper with the designation of the main areas of hydrodynamic pressure.

MEASUREMENT STAND

The measurement stand is presented in Fig. 9, the tested damper being marked with the number '4'. During each test, the damper was filled with silicone oil with a kinematic nominal viscosity $\nu_{25}^{30} = 0.03\ \mathrm{m^2 s^{-1}}$ at a temperature of 25 °C. During the first series of tests, the stand was equipped with a damper without an oil channel. The second series of tests was carried out after modifying the housing and making an oil channel in it. The entire station was driven by an electric squirrel-cage motor marked with the number '1'. The motor power was 0.75 kW and its maximum rotational speed was 1400 rpm, regulated by the motor controller. A two-piston compressor marked with the number '6' was used to generate torsional vibrations. Rigid couplings marked with the number '2' were used to connect all the elements of the stand. Their design guarantees the transfer of torsional vibrations without damping, which is crucial from a measurement point of view. A digital torque meter '5' was placed on the shaft, enabling the recording of the torque with a frequency of up to 2600 Hz. The amplitude-frequency characteristics of the compressor were then determined.

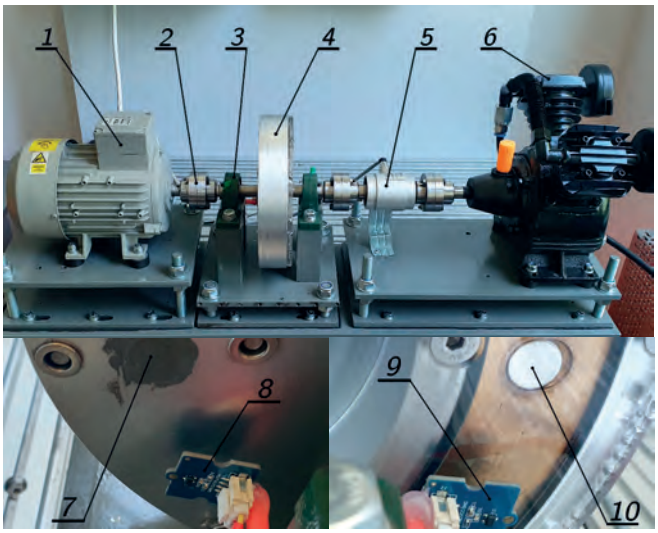

Fig. 9. Measuring stand: 1 - electric motor with adjustable rotational speed, 2 - rigid coupling, 3 - bearing supporting the shaft, 4 - vibration damper, 5 - torque meter, 6 - two-piston compressor for excitation of torsional vibrations, 7 - neodymium magnet in the damper housing, 8 - Hall sensor for the housing, 9 - Hall sensor for the inertia ring, 10 - neodymium magnet in the inertia ring.

The main parts responsible for the measurements are magnets '7' and '10', which are placed in the housing and inertia ring, respectively. The appearance of the magnet in a certain position is registered by the Hall sensors '8' and '9' and this makes it possible to study the relative position of the housing and the inertia ring. The sensors were connected to a recorder with a microcontroller. The system is able to measure the time when the magnet appears in the sensor area with an accuracy of 10^{-5} s. Because of this, it is possible to precisely determine the angular position of both damper elements over time. The recording of the time events takes place asynchronously, based on interruptions generated by the microcontroller's Timer/Counter signals from the sensors. The microcontroller measures the time for full rotation and the time between recording the signal from both Hall sensors. Based on these data, it is possible to determine the relative change in the angular position of the housing and the inertia ring.

RESEARCH RESULTS AND THEIR INTERPRETATION

Experiments were carried out for three rotational speeds of the shaft: n_1 = 426 rpm, n_2 = 702 rpm, and n_3 = 1014 rpm. During the tests, both a damper without a channel and a damper with an oil channel were tested. The time of a single experiment was 1000 s. The damper had a temperature of 25 °C at the beginning of the test and, after its completion, it did not change by more than 1.5 °C. Therefore, it is possible to ignore changes in the viscosity and volume of the silicone oil inside the device.

a) Rotation speed n_1 = 426 rpm.

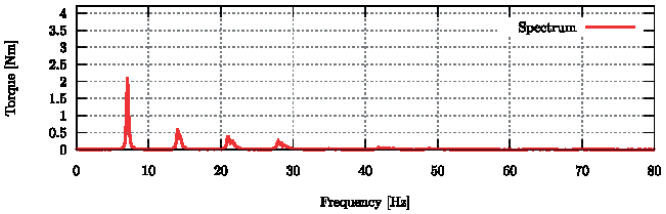

b) Rotation speed n_2 = 702 rpm

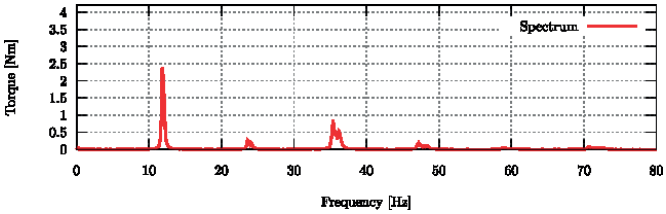

c) Rotation speed n_3 = 1014 rpm

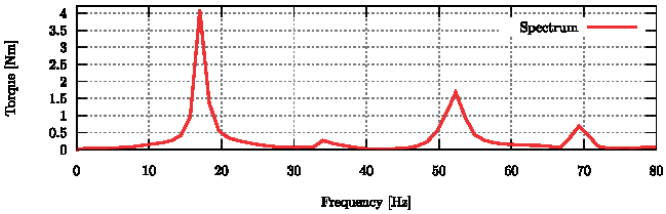

Fig. 10. Spectral characteristics of a two-piston compressor forcing torsional vibrations for individual rotational speeds.

Torsional vibrations were forced by a two-piston compressor; the spectral characteristics for individual rotational frequencies are shown in Fig. 10. The first four harmonics are clearly visible in the spectral image, with the first and third clearly dominating. This is quite natural because the compressor has two pistons and the angle between the cylinders is 90°.

Fig. 11 presents the results of the measurements obtained for rotational speeds $n1$,n_2, and n_3. The graphs show the change in the angular position ϕ of the housing relative to the inertia ring as a function of time. They show that the inertia ring

in the damper without an oil channel in the first phase of the movement performs a follow-up movement relative to the housing. When the oil in the inner carring layer is pushed out in the circumferential direction by the inertia force, the ring stops and does not make any further movement relative to the housing. The relative change in the angular position of the housing and the ring is marked with a red line on the graphs.

a) Rotation speed n_1 = 426 rpm.

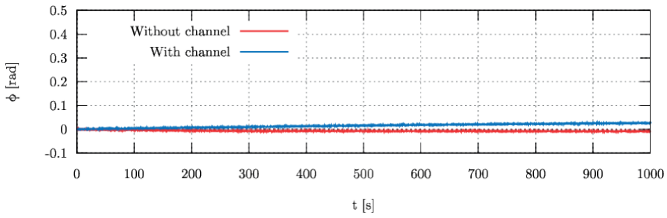

b) Rotation speed n_2 = 702 rpm

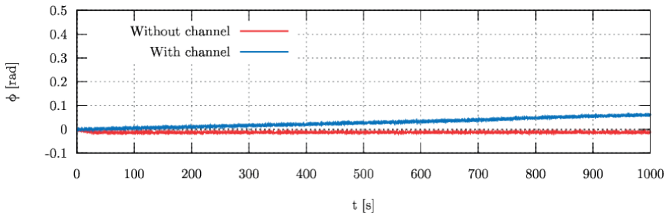

c) Rotation speed n_3 = 1014 rpm

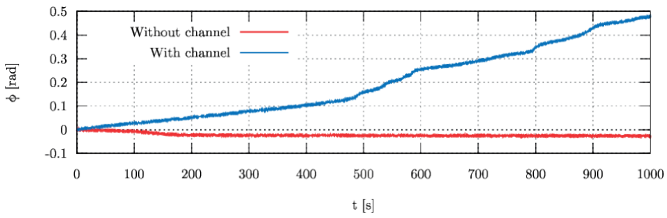

Fig. 11. Graphs of the housing and the inertia ring's relative angular position for a damper without a channel and with an oil channel for different rotation speeds.

The situation is completely different in the case of a damper with an oil channel. In this case, the inertia ring moves in the opposite direction. i.e. it performs an overtaking movement relative to the housing. In addition, the existence of the oil channel means that the inner carrying layer is constantly supplied with oil. Therefore, systematic, relative movement of the inertia ring and housing is observed, which is marked with a blue line in the graphs. This is the state of correct operation of the damper, which dissipates the energy of torsional vibrations through the continuous relative movement of the housing and inertia ring. In Fig. 11c, for a rotational speed of 1014 rpm, there is instability in the increase of the relative angular position ϕ. This results from overheating of the motor due to excessive load and its unstable operation after 500 seconds of the test. The graph shows a large difference between the ϕ variability at 702 rpm and 1014 rpm. For this reason, a decision was made to perform an additional measurement for the rotational speed of 804 rpm. The relationship between ϕ and time t for all four measurements, in the case of a damper with an oil channel, is shown in Fig. 12, which clearly shows the increase in the average relative angular velocity $\overline{\omega} = \frac{\Delta\phi}{\Delta t}$ and this accompanies the increase in rotational speed.

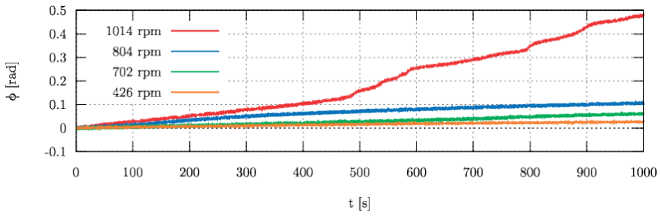

Fig. 12. Plots of the relative angular position of the housing and inertia ring for different rotation speeds.

Table 1 presents the numerical values of the relative position angle ϕ for times t equal to 200, 400, 600, 800 and 1000 s. In addition, the average relative angular velocity $\overline{\omega}$ for the entire test duration and the average relative angular velocity $\overline{\omega}_{200}$ for the time interval [200,1000] is also presented.

The speed $\overline{\omega}_{200}$ is particularly important because it shows how the housing and the inertia ring move relative to each other after the oil is pushed out by the inertia force in the circumferential direction. From the determined values (Table 1), it is clear that in the absence of a channel, the ring practically does not move. In practice, this results in dry or mixed friction between the housing and the inertia ring. During operation, this will lead to excessive wear of the contact surface and damage to the damper. The situation is completely different in the case of a damper with an oil channel. In this case, the movement is visible, which suggests that an oil film has formed that separates the housing from the inertia ring. It should also be noted that the small value of the relative angular velocity justifies the correctness of the assumption

Tab. 1. Numerical summary of selected measurements.

	With channel				Without channel		
rpm	426	702	804	1014	426	702	1014
ϕ(200) rad	0.007	0.010	0.033	0.052	-0.005	-0.014	-0.022
ϕ(200) rad	0.013	0.020	0.062	0.104	-0.006	-0.013	-0.026
ϕ(200) rad	0.018	0.032	0.080	0.255	-0.006	-0.013	-0.026
ϕ(200) rad	0.023	0.047	0.094	0.348	-0.007	-0.012	-0.027
ϕ(200) rad	0.026	0.061	0.106	0.479	-0.007	-0.012	-0.027
$\overline{\omega}$ rad/s	26×10^{-6}	61×10^{-6}	106×10^{-6}	479×10^{-6}	-7×10^{-6}	-12×10^{-6}	-27×10^{-6}
$\overline{\omega}_{200}$ rad/s	24×10^{-6}	64×10^{-6}	91×10^{-6}	534×10^{-6}	-2.5×10^{-6}	2.5×10^{-6}	-6×10^{-6}

about the laminarity of the oil flow. The experimental results therefore confirm that the assumptions made for the model presented in the previous section are correct. It should also be noted that the size of the relative velocity obtained is in line with the results mentioned by Klimczyk et al. [13]. Unfortunately, this two-page publication does not contain detailed numerical information about the results obtained but only focuses on the experiment description, concluding that a single rotation of the inertia ring relative to the housing lasts from several minutes to several hours, depending on the temperature.

CONCLUSIONS REGARDING THE CORRECT DESIGN OF A TORSIONAL VIBRATION VISCOUS DAMPER

As already mentioned, the oil channel is supposed to be a kind of buffer for silicone oil. Therefore, its geometrical parameters, such as depth H and width L (Fig. 8), are strictly dependent on the dimensions of the damper and the temperatures at which it operates. Therefore, we assume that T_F is the damper filling temperature and T_L and T_H are the lowest and highest damper operating temperatures, respectively. In further considerations, we will assume that the damper is filled in thermally stable conditions. This means that both the damper and the oil is filled at a constant temperature T_F. We assume that, in such conditions, the damper can be filled to the degree $\delta \in (0,1)$. This is the part of the volume occupied by the silicone oil at the temperature T_F after the filling process is completed. In general, this factor is approximately 0.9, which means that the damper can be filled to 90%. In addition, we assume that the relative volumetric expansion of silicone oil is independent of temperature and is $\kappa = 0.00093\ °C^{-1}$. By using the introduced notations and modifying the formula given in [3], it is possible to determine the volume occupied by the oil in the viscous damper at a given temperature T:

$$V(T) = V_F(1 + \kappa(T - T_F)) \tag{11}$$

where V_F is the volume of fluid poured into the damper during filling.

As a result of this, it is possible to determine the minimum $V_H = V_F(1 + \kappa\ (T_H - T_F))$ and maximum $V_L = V_F(1 + \kappa\ (T_L - T_F))$ volume that will be occupied by the fluid in the damper. This assumes that the volume of the viscous fluid space in the damper is $V_0 + V$, where V_0 is the volume of the free space around the inertia ring and V is the volume of the oil channel.

From the previous considerations, it follows that

$$V_F = \delta(V_0 + V) \tag{12}$$

$$V_L = \delta(V_0 + V)(1 + \kappa(T_L - T_F)) \tag{13}$$

$$V_H = \delta(V_0 + V)(1 + \kappa(T_H - T_F)) \tag{14}$$

The condition for the formation of an oil film in the inner layer is the fulfillment of the following inequalities: $V_0 < V_L < V_H < V_0 + V$. The inequality $V_L < V_H$ is fulfilled automatically, because the temperature T_L is lower than T_H, which translates into the appropriate relationship for the above volumes. From the inequality $V_H < V_0 + V$ we can derive a dependence:

$$T_H < T_F + \frac{1-\delta}{\kappa\delta} \tag{15}$$

Interestingly, this condition is completely independent of the volume V_0. For silicone oil $\kappa = 0.00093\ °C^{-1}$ and, assuming that the damper is filled to 90% ($\delta = 0.9$), we obtain the condition $T_H < T_F + 119.47$. This means that the maximum operating temperature of the damper cannot exceed the filling temperature by more than 119.47 °C.

From the second inequality $V_0 < V_L$ we obtain the dependence on the minimum volume of the oil channel

$$V > V_0\left(\frac{1}{\delta(1+\kappa(T_L-T_F))} - 1\right) \tag{16}$$

It should be noted that the value in brackets is positive, provided that Eq. (15) and the inequality $T_L < T_H$ are met. Thus, the volume of the oil channel should be an appropriate fraction of the volume V_0. This fraction can be treated as nless function χ of the variable T_F with the parameters δ, κ and T_L.

$$\chi(T_F) = \frac{1}{\delta(1+\kappa(T_L-T_F))} - 1 \tag{17}$$

The graph of the χ function for exemplary parameter values is presented in Fig. 13.

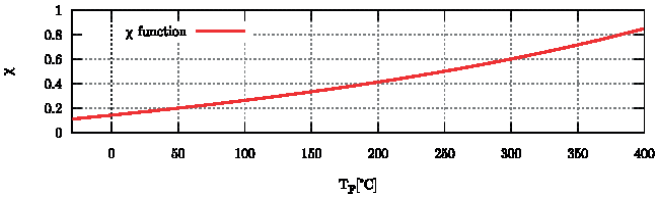

Fig. 13. Graph of the dimensionless function for parameters , and C.

This shows the rate at which the volume of the oil channel increases as a function of the filling temperature. This is especially important for high viscosity silicone oils. In their case, it is necessary to significantly heat the damper and oil so that the injected fluid has the lowest possible viscosity. The numerical value of the volume V_0 is determined on the basis of the geometric parameters of the damper, using the following formula:

$$V_0 = \pi(R_{H,2}^2 - R_{H,1}^2)L_H - \pi(R_{I,2}^2 - R_{I,1}^2)L_I \tag{18}$$

On the other hand, the geometric dimensions H and L of the channel are selected in such a way that they meet the relation $V = \pi HL\ (2R_{H,1} - H)$.

SUMMARY

This article presents a simple analytical model, the task of which is to theoretically justify the reliable operation of a torsional vibration viscous damper. It was found that such a reliable operation requires the formation of an oil film in both gaps of the damper (inner and outer). This model can be the basis for determining the value of the hydrodynamic pressure in a working damper. It also provides the ability to determine the relative position of the housing and the inertia ring. In order to be able to apply this model in a quantitative way, further experimental work is needed to determine the nature of the relative angular velocity.

Next, the authors presented the design and operation of the measuring stand, which was used to test the properties of a medium-size torsional vibration viscous damper. On this stand, a damper made without an oil channel was tested, followed by a modified damper, which already had such a channel. The obtained measurement results clearly show (Fig. 12) that the lack of an oil channel results in stopping the relative movement of the housing and the inertia ring. In practice, this means that there is no vibration damping. The use of a transparent cover also made it possible to show how the force of inertia pushes the oil towards the outer gap.

In summary, the authors derived analytical equations for the volume of the oil channel, which would guarantee the correct formation of an oil film in both carrying layers. The volume of the channel can be calculated as the product of the free space for oil and a certain dimensionless characteristic function . This function was introduced by the authors and depends on four values: the lowest damper operating temperature, the damper filling temperature, the degree of filling of the damper and the relative volumetric expansion of the viscous fluid (in this case, silicone oil).

REFERENCES

1. D. Baranovskyi, S. Myamlin, M. Bulakh, D. Podosonov, and L. Muradian, 'Determination of the Filler Concentration of the Composite Tape', Applied Sciences. vol. 12, no. 21, 11044, 2022. doi: 10.3390/app122111044

2. P. Charles, J. Sinha, F. Gu, L. Lidstone, and A. Ball, 'Detecting the crankshaft torsional vibration of diesel engines for combustion related diagnosis', Journal of sound and vibration, vol. 321, no. 3-5, pp. 1171-1185, 2009. doi: 10.1016/j.jsv.2008.10.024

3. A. Chmielowiec, W. Woś, and J. Gumieniak, 'Viscosity Approximation of PDMS Using Weibull Function', Materials, vol. 14, no. 20, 6060, 2021. doi: 10.3390/ma14206060

4. J. Dziurdź and R. Pakowski, 'Analysis of action viscous torsional vibration damper of the crankshaft based on transverse vibration the engine block', in Solid State Phenomena, vol. 236, pp. 145-152, 2015. doi: 10.4028/www.scientific.net/SSP.236.145

5. M. Fonte and M. De Freitas, 'Marine main engine crankshaft failure analysis: a case study', Engineering Failure Analysis, vol. 16, no. 6, pp. 1940-1947, 2009. doi: 10.1016/j.engfailanal.2008.10.013

6. M. Fonte, P. Duarte, V. Anes, M. Freitas, and L. Reis, 'On the assessment of fatigue life of marine diesel engine crankshafts', Engineering failure analysis, vol. 56, pp. 51-57, 2015. doi: 10.1016/j.engfailanal.2015.04.014

7. J. Gomes, N. Gaivota, R. Martins, and P. Silva, 'Failure analysis of crankshafts used in maritime V12 diesel engines', Engineering Failure Analysis, vol. 92, pp. 466-479, 2018. doi: 10.1016/j.engfailanal.2018.06.020

8. H. Han, K. Lee, and S. Park, 'Parametric study to identify the cause of high torsional vibration of the propulsion shaft in the ship', Engineering Failure Analysis, vol. 59, pp. 334-346, 2016. doi: 10.1016/j.engfailanal.2015.10.018

9. W. Homik, 'Diagnostics, maintenance and regeneration of torsional vibration dampers for crankshafts of ship diesel engines', Polish Maritime Research, vol. 17, no. 1, pp. 62-68, 2010. doi: 10.2478/v10012-010-0007-2

10. W. Homik, 'Damping of torsional vibrations of ship engine crankshafts-general selection methods of viscous vibration damper', Polish Maritime Research, vol. 18, no. 3, pp. 43-47, 2011. doi: 10.2478/v10012-011-0016-9

11. W. Homik, 'The effect of liquid temperature and viscosity on the amplitude-frequency characteristics of a viscotic torsion damper', Polish Maritime Research, vol. 19, no. 4, pp. 71-77, 2012. doi: 10.2478/v10012-012-0042-2

12. Y. Hori,'Hydrodynamic Lubrication'. Springer, Tokyo, 2006. doi: 10.1007/4-431-27901-6

13. S. Klimczyk, A. Szymański, and A. Lipiński, 'Isotope method for determining the displacement of the inertia ring of a torsional vibration damper' (in Polish), in Fizyka dla przemysłu - materiały V konferencji, Poznań, pp. 114-115, 1986.

14. T. Kodama and Y. Honda, 'Study on torsional vibration characteristics of small high-speed marine diesel engine crankshaft system with viscous friction damper: Numerical calculation method of torsional angular displacement and stress using simultaneous measurement values at two points', Journal of the Korean Society of Marine Engineering, vol. 41, no. 8, pp. 723-731, 2017. doi: 10.5916/jkosme.2017.41.8.723

15. T. Kodama and Y. Honda, 'A Study on the Modeling and Dynamic Characteristics of the Viscous Damper Silicone Fluid Using Vibration Control of Engine Crankshaft Systems', International Journal of Mechanical Engineering and Robotics Research, vol. 7, no. 3, 2018. doi: 10.18178/ijmerr.7.3.273-278

16. S. Kutay and B. Kamal, 'Assessment of marine diesel engine crankshaft damages', Ships and Offshore Structures, vol. 17, no. 9, pp. 2130-2139, 2022. doi: 10.1080/17445302.2022.2050522

17. R. Liberacki, 'Risk criteria for sea-going ships arising from the operation of the main engines' crankshaft-connecting rod-piston systems', Journal of Polish CIMAC, vol. 7, no. 2, pp. 115-121, 2012.

18. L. Murawski, 'Axial vibrations of the ship power transmission system: propulsion shaftline engine crankshaft', Polish Maritime Research, vol. 3, no. 9, pp. 21-28, 1996.

19. L. Murawski and M. Dereszewski, 'Theoretical and practical backgrounds of monitoring system of ship power transmission systems' torsional vibration', Journal of Marine Science and Technology, vol. 25, no. 1, pp. 272-284, 2020. doi: 10.1007/s00773-019-00646-z

20. M. Pasricha, 'Effect of damping on parametrically excited torsional vibrations of reciprocating engines including gas forces', Journal of ship research, vol. 50, no. 02, pp. 147-157, 2006. doi: 10.5957/jsr.2006.50.2.147

21. O. Reynolds, 'On the Theory of Lubrication and its Application to Mr.B. Tower's Experiments', Philosophical Transaction of Royal Society of London, vol. 177, no. 1, pp. 157-234, 1886.

22. I. Senjanović, N. Hadzić, L. Murawski, N. Vladimir, N. Alujević, and D.-S. Cho, 'Analytical procedures for torsional vibration analysis of ship power transmission system', Engineering Structures, vol. 178, pp. 227-244, 2019. doi: 10.1016/j.engstruct.2018.10.035